Pergamon

PII: S0094-114X(96)00043-2

Mech. Mach. Theory Vol. 32, No. 2, pp. 121–136, 1997

0094-114X/97 $17.00 + 0.00

MATHEMATICAL MODEL OF SPIRAL BEVEL AND HYPOID GEARS MANUFACTURED BY THE MODIFIED ROLL METHOD

CHUNG-YUNN LIN and CHUNG-BIAU TSAY

Department of Mechanical Engineering, National Chiao Tung University, Hsinchu, Taiwan 30050, Republic of China

ZHANG-HUA FONG

Department of Mechanical Engineering, National Chung Cherng University, Chia-Yi, Taiwan 62101, Republic of China

(Received 30 October 1995)

Abstract—Based on grinding mechanism and machine-tool settings of the Gleason modified roll hypoid grinder, a mathematical model for the tooth geometry of spiral bevel and hypoid gears is developed. Since all the machine-tool settings and machine constants are involved in the proposed mathematical model, excellent correlation between the mathematical model and actual manufacturing machines can be obtained. An example is given to illustrate the application of the proposed mathematical model. Surface deviation between a real cut spiral bevel gear surface and the model surface is investigated. Bearing contacts and kinematic errors in the spiral bevel gear set are also studied. Copyright ©1996 Elsevier Science Ltd

1. INTRODUCTION

There are several important systems for the manufacture of circular-cut spiral bevel and hypoid gears, for example, the spread blade-fixed setting method with a modified roll machine, the spherical duplex method, the helical duplex method, the spread blade-fixed setting method with tilted cutter axis, the helixform method and the formate method. Spiral bevel and hypoid gears manufactured by the helixform method and formate method have been proposed by the Gleason Works [1], Baxter [2] and Litvin and Gutman [3]. Huston and Coy [4], Huston *et al.* [5] proposed mathematical models for logarithmic spiral bevel gears in 1981 and for circular-cut spiral bevel gears in 1983. Tsai and Chin [6] investigated the surface geometry of straight and spiral bevel gears in 1987. In 1988, Litvin *et al.* [7] proposed a method for determining the machine-tool settings for the machine cradle of a tilted head cutter. Fong and Tsay [8–11] presented a series of papers to investigate spiral bevel gear surface geometry, cutting machine mechanisms, kinematic characteristics and undercutting effects.

Recent technological development on the CNC machinery makes it possible to manufacture and inspect spiral and hypoid gears under full quantitative and qualitative controls. Several computer-aided CNC inspection systems and closed loop manufacturing systems, that combine CNC coordinate measuring machines and theoretical gear surface data, for bevel and hypoid gears have been developed by the Gleason Works [12], M&M Precision Systems [13], Klingelnberg Soehne [14] and Lemanski [15] in the past few years. Krenzer [16] proposed computer-aided corrective machine settings for bevel and hypoid gears manufacturing that use first-order and second-order sensitivity matrices. Litvin *et al.* [17–19] also proposed a series of methodologies for minimizing surface deviations and analyzing the meshing and contact of real cut gear tooth surfaces using coordinate measuring machines.

Since the tooth surface geometries of spiral bevel and hypoid gears are quite complex and vary with the manufacturing method, accurate data calculation of theoretical tooth surfaces is difficult for engineers wanting to establish CNC inspection systems for spiral bevel and hypoid gears. Therefore, it is desirable to investigate theoretical tooth surface calculations of spiral bevel and hypoid gears as manufactured by different systems.

In this paper, a mathematical model for spiral bevel and hypoid gears manufactured by the Gleason modified roll method [20–23] is proposed. To guarantee close correlation between the mathematical model and actual manufacturing machine, the proposed mathematical model for spiral bevel and hypoid gears is developed based on the mechanism of Gleason no. 463 series hypoid grinder. The generating train of the Gleason no. 463 hypoid grinder is designed to perform the modified roll motion by means of a special cam reciprocator mechanism. The kinematic characteristics of the hypoid grinder are grouped into four modules: (a) surface geometry of cup-shaped grinding wheel; (b) special modified roll generating train; (c) spatial relationship between the workpiece and the grinding wheel; and (d) equation of meshing that simulates the grinding generation process.

Since the proposed mathematical model for spiral bevel and hypoid gears is derived in terms of actual machine-tool settings and machine constants, it is very easy to implement the mathematical model and to establish a closed loop manufacturing system for spiral bevel and hypoid gears. Many computer problems such as the tooth contact analysis (TCA) program, computer-aided CNC inspection program and corrective machine-tool settings calculation program have been developed and can be used to form a closed loop manufacturing system. An example is given to illustrate application of the proposed mathematical model. Surface deviation between the real cut spiral bevel gear and the proposed mathematical model has been investigated. Bearing contacts and kinematic errors in the sprial bevel gear have also been studied.

2. MATHEMATICAL MODEL FOR THE GLEASON SPIRAL BEVEL AND HYPOID GEARS

2.1. Surface geometry of the cup-shaped grinding wheel

The surface geometry of the face mill cutter and the cup-shaped grinding wheel is usually considered a cone surface as shown in Fig. 1 [8, 9]. The axial cross-section of the cup-shaped grinding wheel is straight-edged in the a–a cross-section in Fig. 1. The position vector and unit normal vector of the cup-shaped grinding wheel surface can be represented by [9]:

$$\mathbf{R}_1(u_j, \beta_j) = \begin{Bmatrix} x_1 \\ y_1 \\ z_1 \\ 1 \end{Bmatrix} = \begin{Bmatrix} \left[r_m \pm \left(\frac{W}{2} + u_j \sin \psi_j \right) \right] \sin \beta_j \\ \left[r_m \pm \left(\frac{W}{2} + u_j \sin \psi_j \right) \right] \cos \beta_j \\ -u_j \cos \psi_j \\ 1 \end{Bmatrix}, \tag{1}$$

and

$$\mathbf{n}_j = \frac{\mathbf{N}_j}{|\mathbf{N}_j|},$$

where

$$\mathbf{N}_j = \frac{\partial \mathbf{R}_j}{\partial u_j} \times \frac{\partial \mathbf{R}_j}{\partial \beta_j}, \quad \text{and} \quad j = \text{i, o}.$$

The subscripts "i" and "o" denote the inside and outside blades, respectively. The "$\pm$" sign should be considered a "+" sign for the outside blade and a "−" sign for the inside blade. Parameters u_i, β_i, u_o, and β_o are the surface coordinates of the inside and outside blades, respectively.

Actually, the axial cross-section of the grinding wheel need not necessarily be straight-edged. Other cross-sections can be used for special manufacturing systems such as the spherical duplex system. In such cases, equation (1) should be modified according to the corresponding cross-section geometry.

2.2. *The modified roll generating train*

The roll ratio between the imaginary generating gear and the workpiece is not a constant during the generation process of the modified roll method. As shown in Fig. 2(a), the timing relationship between the workpiece and the imaginary generating gear is determined by the positive cam-follower reciprocator mechanism and the index change gears of the Gleason no. 463 hypoid grinder. The instantaneous roll ratio η_a between the imaginary generating gear and the workpiece can be expressed by

$$\eta_a = \frac{\xi_w}{\xi_c} = \frac{T_i}{T_p} R_a, \tag{2}$$

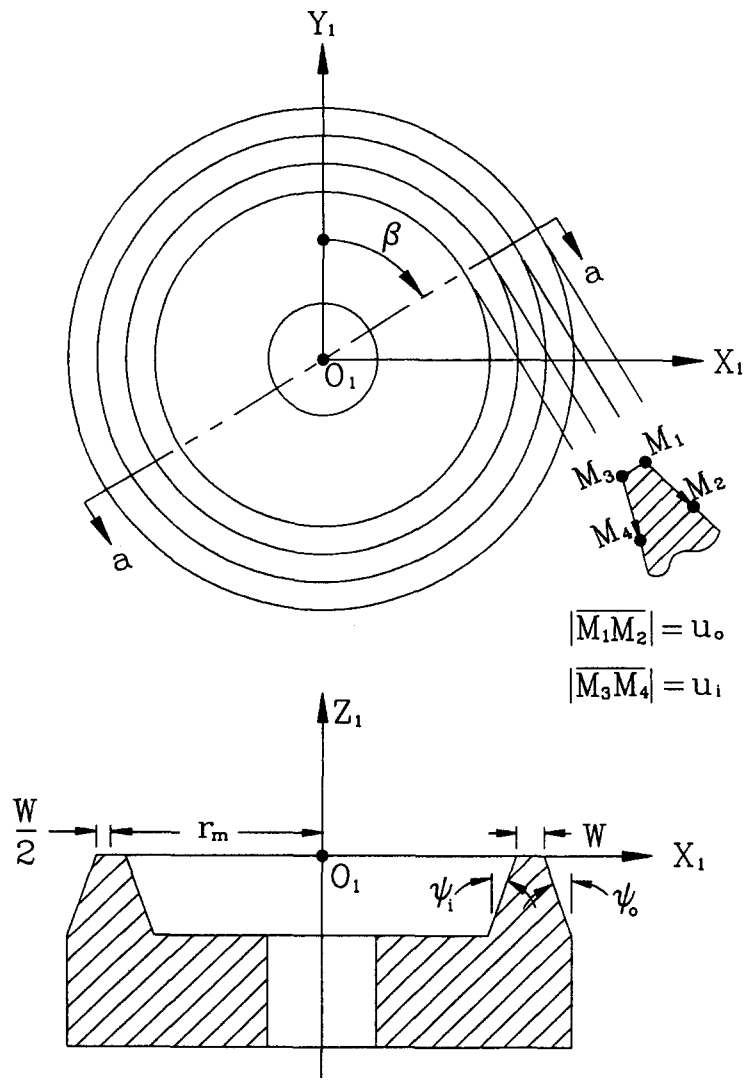

Fig. 1. Coordinate system S_1 and geometry of the cup-shaped grinding wheel.

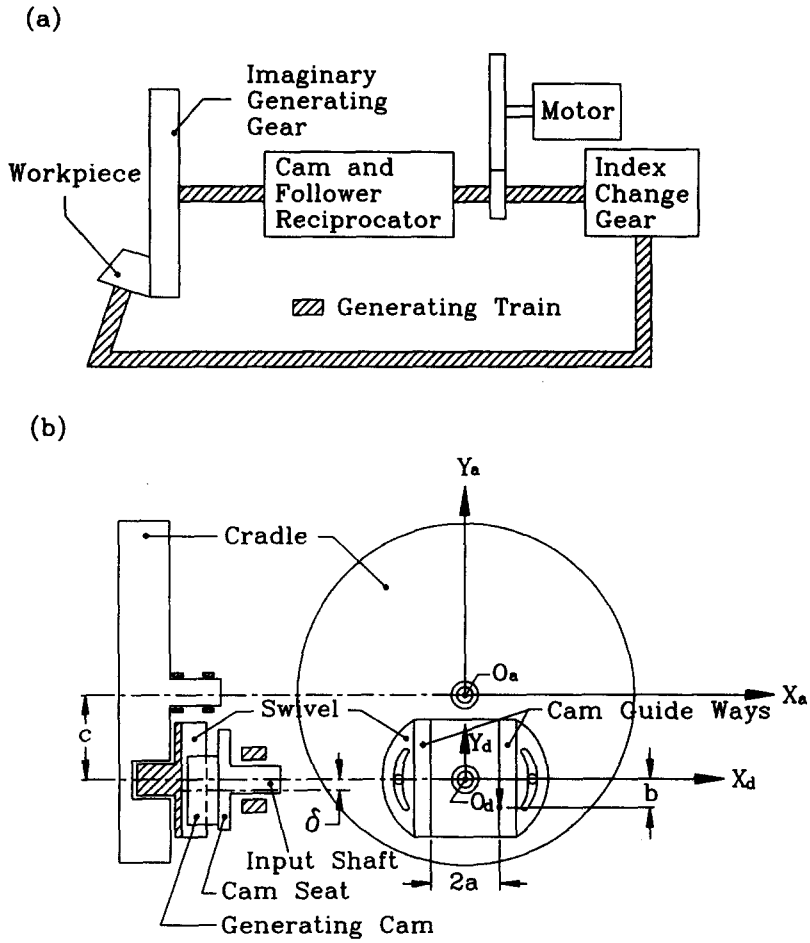

Fig. 2. The modified roll generating train of the Gleason no. 463 hypoid grinder: (a) generating trains; (b) cam follower and reciprocator.

where ξ_w is the work spindle rotation angle, ξ_c is the cradle rotation angle, R_a is the instantaneous roll ratio of the cam-follower reciprocator and T_i and T_p are the tooth numbers of the index interval and pinion, respectively. The total gear ratio of the index change gears is equal to the ratio of T_i/T_p. As shown in Fig. 2(b), the cradle reciprocating motion is achieved by the resultant motion of the generating cam and the captive swivel. The generating train rotates at a constant rotational speed with respect to the input shaft, which is coupled to the work spindle through the index changer gears. The generating cam is mounted on the input shaft with a cam seat. By adjusting the cam setting on the cam seat, the generating cam can be displaced with respect to the rotational center of the input shaft O_d by a predetermined distance δ, which is a machine setting for the hypoid grinder. The captive swivel has two straight and parallel cam guide ways. The swivel is also mounted on the cradle and the rotational angle of the swivel with respect to the cradle is defined as the cam guide angle φ, as shown in Fig. 3. The rotational center of the swivel O_d is lower than that of the cradle center O_a by distance C, which is a machine constant. The rotational center of the input shaft O_d is also assembled lower than the cradle center O_a by the same distance C. The generating cam is in constant contact with the cam guide ways on both sides. Therefore, the cradle's reciprocating motion is achieved by the constant-breadth generating cam and the captive swivel. The instantaneous rotational speed and rotational angle of the machine cradle are determined by the profile and position of the generating cam, cam guide angle φ, cam setting δ, as well as the gear ratio of index change gears.

The instantaneous roll ratio R_a between the input shaft and the cradle can be derived according to the following two kinematic requirements:

(1) If the cam guide angle φ and cam setting δ are zeros, the instantaneous roll ratio R_a between cradle and input shaft is constant during the generation process. Accordingly, the profile of the generating cam can be obtained by considering the conjugate motion between straight cam guide ways and generating cam.

(2) By applying equations of the generating cam and constant contact conditions between generating cam and captive swivel, the instantaneous roll ratio R_a between input shaft and cradle can be derived in terms of the cam guide angle φ and cam setting δ.

The coordinate systems for profile derivation of the generating cam are shown in Fig. 3. Coordinate systems $S_b(x_b, y_b)$ and $S_c(x_c, y_c)$ are rigidly attached to the grinding machine frame while coordinate systems $S_a(x_a, y_a)$, $S_d(x_d, y_d)$, $S_e(x_e, y_e)$ and $S_f(x_f, y_f)$ are rigidly attached to the cradle, swivel, generating cam and input shaft, respectively. The generating cam profile can be determined based on the following consideration:

If the cam guide angle φ and cam setting δ are zeros, the roll ratio between cradle and input shaft during the generating process can be viewed as simply two internally contacting circles. The pitch radius of the generating cam is defined as r_u and the distance between the cradle center O_a and the rotational center of input shaft O_f is C. Therefore, the instantaneous roll ratio R_a between the input shaft and cradle can be expressed by:

$$R_a = \left(\frac{d\alpha_e}{d\alpha_a}\right) = \frac{C + r_u}{r_u}, \quad \text{when } \delta = 0 \text{ and } \varphi = 0; \tag{3}$$

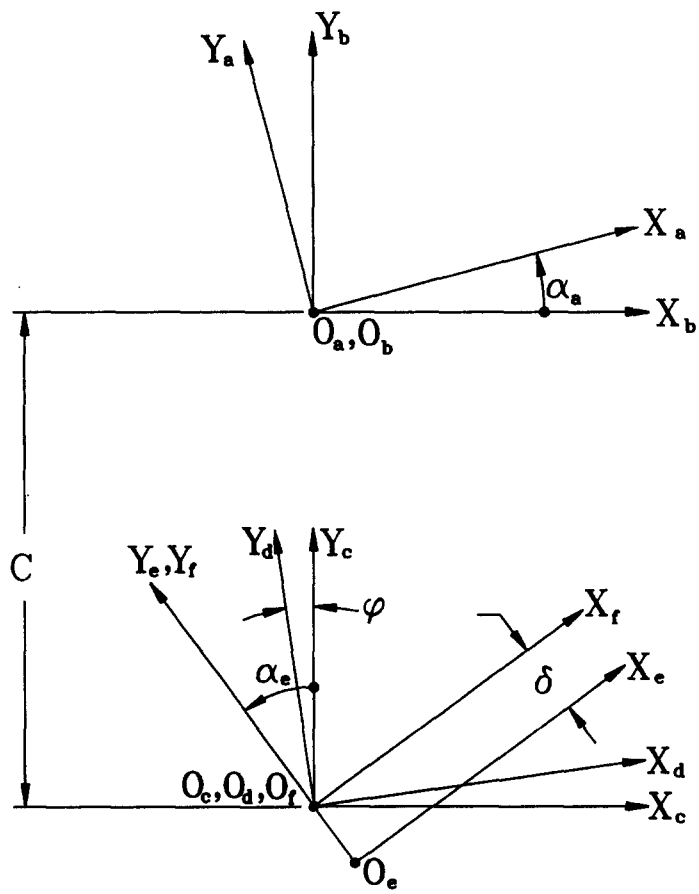

Fig. 3. Relationships among coordinate systems S_a, S_b, S_c, S_d, S_e and S_f.

α_a and α_e are the rotational angles of the cradle and input shaft, respectively. The generating cam profile can be obtained by finding the cam guide ways' motion envelopes. The locus of the cam guide ways represented in coordinate system $S_e(x_e, y_e)$ is obtained by

$$\begin{Bmatrix} x_e \\ y_e \\ 1 \end{Bmatrix} = [M_{ea}] \begin{Bmatrix} x_a \\ y_a \\ 1 \end{Bmatrix}, \quad \text{when } \delta = 0 \text{ and } \varphi = 0$$

$$= \begin{bmatrix} \cos(\alpha_a - \alpha_e) & -\sin(\alpha_a - \alpha_e) & C \sin \alpha_e \\ \sin(\alpha_a - \alpha_e) & \cos(\alpha_a - \alpha_e) & C \cos \alpha_e \\ 0 & 0 & 1 \end{bmatrix} \begin{Bmatrix} a \\ b - C \\ 1 \end{Bmatrix}, \tag{4}$$

where "a" is the half distance between two cam guide ways and parameter "b" is a surface coordinate on the cam guide ways, as shown in Fig. 2. The unit normal vector of the locus of the cam guide ways is

$$\begin{Bmatrix} n_{xe} \\ n_{ye} \end{Bmatrix} = \begin{Bmatrix} \cos(\alpha_a - \alpha_e) \\ \sin(\alpha_a - \alpha_e) \end{Bmatrix}, \quad \text{when } \delta = 0 \text{ and } \varphi = 0. \tag{5}$$

Conjugate motion between the cam guide ways and the generating cam can be obtained by applying the equation of meshing [22], i.e. the common normal vector of the cam guide ways and generating cam should always be perpendicular to their relative velocity at every contact point. Based on this conjugate motion condition, the final formula for the equation of meshing between the cam guide ways and generating cam becomes

$$(b - C) = -(C + r_u)\cos \alpha_a, \quad \text{when } \delta = 0 \text{ and } \varphi = 0; \tag{6}$$

r_u is the pitch radius of the generating cam. Therefore, equations for the generating cam can be derived by substituting equations (3) and (6) into equation (4). To distinguish the generating cam surface coordinates from the variable rotational angle, the subscript of α_a is dropped when the variable represents the generating cam surface coordinates. Therefore, the generating cam profile can be expressed by

$$\mathbf{R}_e(\alpha) = \begin{Bmatrix} x_e(\alpha) \\ y_e(\alpha) \\ 1 \end{Bmatrix} = \begin{Bmatrix} a \cos\left(-\frac{C}{r_u}\alpha\right) + (C + r_u)\cos \alpha \sin\left(-\frac{C}{r_u}\alpha\right) + C \sin\left(\frac{C + r_u}{r_u}\alpha\right) \\ a \sin\left(-\frac{C}{r_u}\alpha\right) - (C + r_u)\cos \alpha \cos\left(-\frac{C}{r_u}\alpha\right) + C \cos\left(\frac{C + r_u}{r_u}\alpha\right) \\ 1 \end{Bmatrix}. \tag{7}$$

Thus, the generating cam profile is defined in terms of the surface coordinate α. The unit normal vector of the generating cam becomes

$$\begin{Bmatrix} n_{xe}(\alpha) \\ n_{ye}(\alpha) \end{Bmatrix} = \begin{Bmatrix} \cos\left(-\frac{C}{r_u}\right) \\ \sin\left(-\frac{C}{r_u}\right) \end{Bmatrix}. \tag{8}$$

The singular point of equation (7) can be found by letting $dx_e/d\alpha = dy_e/d\alpha = 0$, i.e. the singular point exists when

$$\alpha = \sin^{-1}\left(\frac{aC}{r_u^2 - C^2}\right). \tag{9}$$

The maximum uniform roll angle between the input shaft and cradle is thus constrained by equation (9).

Since the profiles of the generating cam and cam guide ways are known, the time relationship between the input shaft and cradle can be determined by the constant contact condition between the generating cam and cam guide ways. In other words, the surface position vectors and surface unit normal vectors of the generating cam and cam guide ways should be the same at the contact point. However, both position and unit normal vectors of the mating surfaces should be expressed in the same coordinate system, say, the S_c coordinate system. According to the coordinate systems shown in Fig. 3, the position and unit normal vectors of the generating cam and cam guide ways can be expressed in coordinate system $S_c(x_c, y_c)$ as follows:

$$\mathbf{R}_c^g = \begin{Bmatrix} x_c^g \\ y_c^g \\ 1 \end{Bmatrix} = \begin{bmatrix} \cos\alpha_e & -\sin\alpha_e & 0 \\ \sin\alpha_e & \cos\alpha_e & 0 \\ 0 & 0 & 1 \end{bmatrix} \begin{Bmatrix} x_e \\ y_e - \delta \\ 1 \end{Bmatrix}, \tag{10}$$

$$\mathbf{R}_c^w = \begin{Bmatrix} x_c^w \\ y_c^w \\ 1 \end{Bmatrix} = \begin{bmatrix} \cos\alpha_a & -\sin\alpha_a & 0 \\ \sin\alpha_a & \cos\alpha_a & C \\ 0 & 0 & 1 \end{bmatrix} \begin{bmatrix} \cos\varphi & \sin\varphi & 0 \\ -\sin\varphi & \cos\varphi & -C \\ 0 & 0 & 1 \end{bmatrix} \begin{Bmatrix} a \\ b \\ 1 \end{Bmatrix}, \tag{11}$$

$$\mathbf{n}_c^g = \begin{Bmatrix} n_{xc}^g \\ n_{yc}^g \end{Bmatrix} = \begin{Bmatrix} \cos\left(-\frac{C}{r_u}\alpha\right)\cos\alpha_e - \sin\left(-\frac{C}{r_u}\alpha\right)\sin\alpha_e \\ \cos\left(-\frac{C}{r_u}\alpha\right)\sin\alpha_e + \sin\left(-\frac{C}{r_u}\alpha\right)\cos\alpha_e \end{Bmatrix}, \tag{12}$$

and

$$\mathbf{n}_c^w = \begin{Bmatrix} n_{xc}^w \\ n_{yc}^w \end{Bmatrix} = \begin{Bmatrix} \cos\alpha_a\cos\varphi + \sin\alpha_a\sin\varphi \\ \sin\alpha_a\cos\varphi - \cos\alpha_a\sin\varphi \end{Bmatrix}, \tag{13}$$

where superscript "w" denotes the cam guide ways and superscript "g" denotes the generating cam. Subscript "c" denotes that the vector is represented in coordinate system S_c. The time relationship between the cradle and input shaft can be obtained by letting:

$$\mathbf{R}_c^g = \mathbf{R}_c^w, \tag{14}$$

and

$$\mathbf{n}_c^g = \mathbf{n}_c^w. \tag{15}$$

Since equation (15) is constrained by $|\mathbf{n}_c^g| = |\mathbf{n}_c^w| = 1$, equations (14) and (15) imply three scalar equations with four variables: b, α, α_a, and α_e. The time relationship between α_a and α_e can be solved by eliminating α and b as follows:

$$\alpha = \frac{r_u}{C}(\alpha_e - \alpha_a + \varphi), \tag{16}$$

and

$$b = \frac{(r_u + C)\sin(\alpha_a - \varphi + \alpha) + (r_u - C)\sin(\alpha_a - \varphi - \alpha) - 2C\sin\alpha_a + 2\delta\sin\alpha_e}{2\sin(\varphi - \alpha_a)}. \tag{17}$$

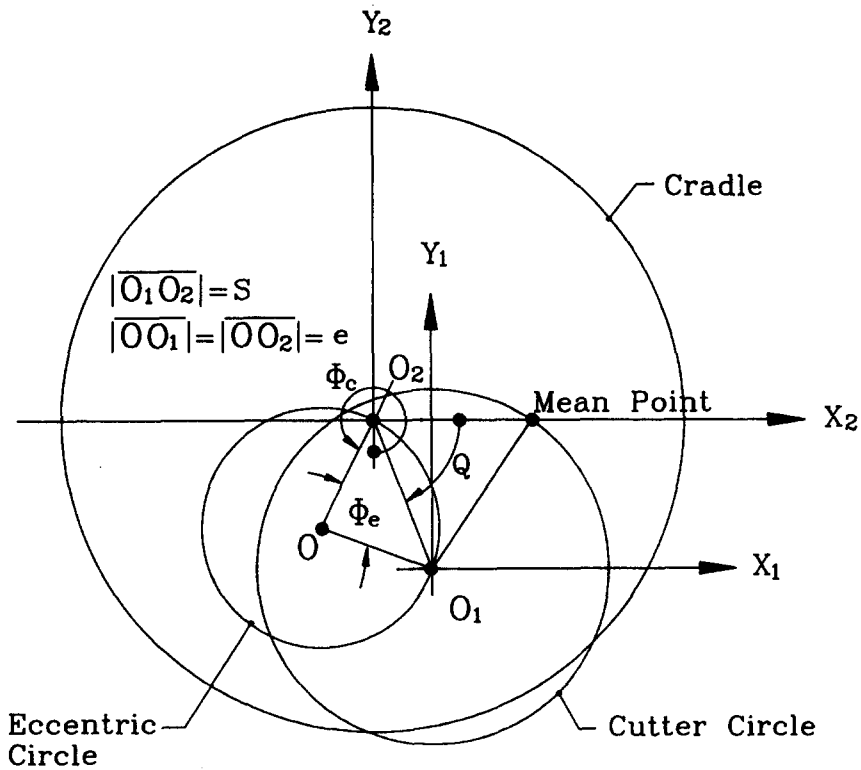

Fig. 4. Relationships among machine settings and basic cradle settings.

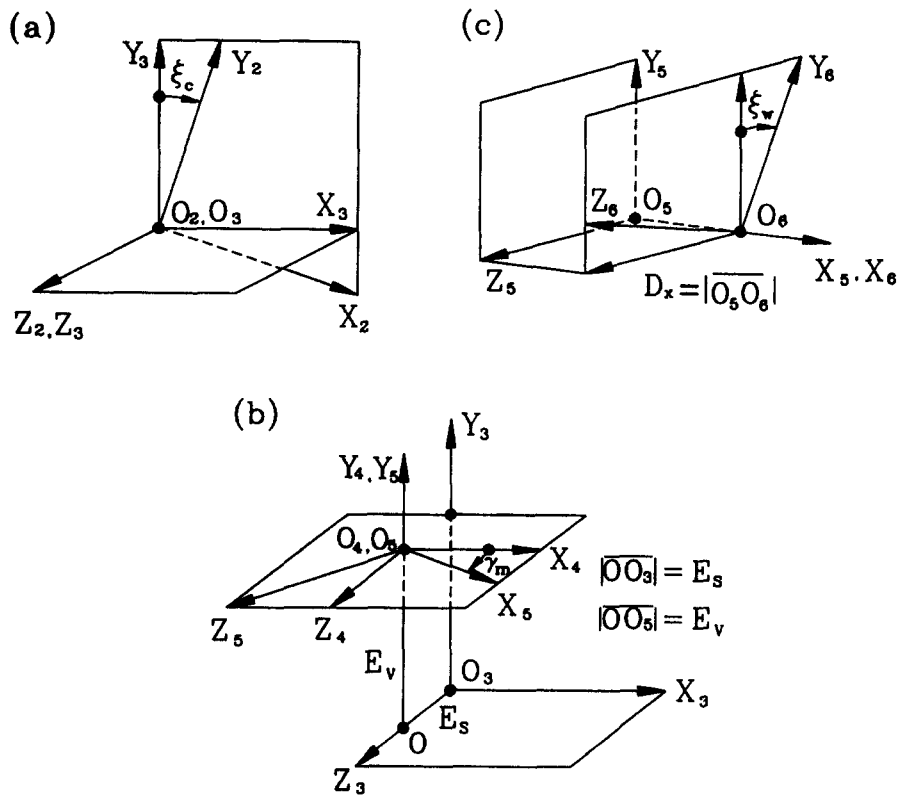

Fig. 5. Coordinate systems for the bevel gear generation mechanism.

By substituting equations (16) and (17) into equations (14) and (15), the constant contact condition between generating cam and cam guide ways can be reduced to only one scalar equation as follows:

$$f(\alpha_a, \alpha_e) = C\left\{\sin\varphi + \sin\left[\frac{r_u}{C}(\alpha_a - \alpha_e - \varphi)\right] + \sin(\alpha_a - \varphi)\right\} + \delta\sin(\alpha_a - \alpha_e - \varphi) = 0. \quad (18)$$

Thus, the instantaneous roll ratio R_a between the input shaft and cradle is obtained by the following differentiation:

$$R_a(\alpha_a, \alpha_e) = \frac{d\alpha_e}{d\alpha_a} = -\frac{f_{\alpha_a}}{f_{\alpha_e}} = \frac{C\cos(\alpha_a - \varphi)}{\alpha\cos(\alpha_e - \alpha_a + \varphi) + r_u\cos\left[\frac{r_u}{C}(\alpha_e - \alpha_a + \varphi)\right]} + 1. \quad (19)$$

2.3. The spatial relationship between the imaginary generating gear and the workpiece

The spatial relationship between the imaginary gear and the workpiece is shown in Figs 4 and 5. The Modified Roll Method cutter spindle is parallel to the cradle axis. Based on the geometry shown in Fig. 4, the tooth surface and surface unit normal of the imaginary generating gear can be represented as follows:

$$Q = 360^\circ - \phi_c + \frac{\phi_e}{2}, \quad (20)$$

$$S = 2e\sin\left(\frac{\phi_e}{2}\right), \quad (21)$$

$$\mathbf{R}_2 = \begin{Bmatrix} x_2 \\ y_2 \\ z_2 \\ 1 \end{Bmatrix} = \begin{Bmatrix} S\cos Q + x_1 \\ -S\sin Q + y_1 \\ z_1 \\ 1 \end{Bmatrix}, \quad (22)$$

and $\mathbf{n}_2 = \mathbf{n}_1$, where

ϕ_c is the cradle angle and is one of the machine settings for the Gleason hypoid grinder;
ϕ_e is the eccentric angle and is also a machine setting;
e is the machine constant of eccentric, e = 8 inches for the Gleason no. 463 hypoid grinder;
S is the basic radial distance setting;
Q is the basic cradle angle setting;

and, x_1, y_1 and z_1 are the surface coordinates of the cup-shaped grinding wheel represented in equation (1).

As shown in Fig. 5 [9], coordinate systems $S_2(x_2, y_2, z_2)$, $S_3(x_3, y_3, z_3)$, $S_4(x_4, y_4, z_4)$, $S_5(x_5, y_5, z_5)$ and $S_6(x_6, y_6, z_6)$ are rigidly attached to the cradle, machine frame, sliding base, work head and workpiece, respectively. Therefore, the locus of the imaginary generating gear represented in the workpiece coordinate system S_6 can be obtained by applying the following coordinate transformation matrix equation:

$$\mathbf{R}_6 = [M_{65}][M_{53}][M_{32}]\mathbf{R}_2, \quad (23)$$

where

$$[M_{65}] = \begin{bmatrix} 1 & 0 & 0 & -D_x \\ 0 & \cos\xi_w & -\sin\xi_w & 0 \\ 0 & \sin\xi_w & \cos\xi_w & 0 \\ 0 & 0 & 0 & 1 \end{bmatrix},$$

$$[M_{53}] = \begin{bmatrix} \cos\gamma_m & 0 & \sin\gamma_m & -E_s\sin\gamma_m \\ 0 & 1 & 0 & -E_v \\ -\sin\gamma_m & 0 & \cos\gamma_m & E_s\cos\gamma_m \\ 0 & 0 & 0 & 1 \end{bmatrix},$$

$$[M_{32}] = \begin{bmatrix} \cos\xi_c & \sin\xi_c & 0 & 0 \\ -\sin\xi_c & \cos\xi_c & 0 & 0 \\ 0 & 0 & 1 & 0 \\ 0 & 0 & 0 & 1 \end{bmatrix};$$

ξ_c is the cradle rotational angle;
ξ_w is the work spindle rotational angle;
γ_m is the machine root angle;
D_x is the increment of machine center to back;
E_s is the sliding base setting;
E_v is the vertical offset setting.

The cradle rotational angle ξ_c and work spindle rotational angle ξ_w can be represented in terms of the generating cam surface coordinate α as follows:

$$\xi_c(\alpha) = \varphi + \sin^{-1}\left[\frac{\delta}{C}\sin\left(\frac{C\alpha}{r_u}\right) + \sin\alpha - \sin\varphi\right], \tag{24}$$

and

$$\xi_w(\alpha) = \frac{n_i}{n_p}\left(\frac{C\alpha}{r_u} + \xi_c - \varphi\right). \tag{25}$$

2.4. Equation of meshing

The generation process during modified roll cutting or grinding can be simulated by considering the equation of meshing [9] and the kinematic relationship between the imaginary generating gear and the workpiece, simultaneously. Due to the tangency of two mating surfaces, the relative velocity of mating surfaces must lie on the common tangent plane during the generating process. Therefore, the following equation must be observed:

$$\mathbf{n} \cdot \mathbf{V}_{12} = 0, \tag{26}$$

where $\mathbf{n}$ is the unit normal vector of the generating tool surface and $\mathbf{V}_{12}$ is the relative velocity between the generating tool surface and the generated gear blank surface. It is worth mentioning that equation (26) is the so-called "equation of meshing" in the theory of gearing. After some mathematical manipulations, equation (26) becomes

$$A + B\sin\xi_c + C\cos\xi_c = 0, \tag{27}$$

where

$$AA = \left(\sin\gamma_m - \frac{1}{\eta_a}\right)(y_2 n_{x2} - x_2 n_{y2}) + n_{z2} E_v \cos\gamma_m,$$

$$BB = -E_v n_{y2} \sin\gamma_m - [n_{x2}(z_2 - E_s) - x_2 n_{z2}]\cos\gamma_m,$$

and

$$CC = -E_v n_{x0} \sin\gamma_m + \left[n_{y0}\left(z_0 - E_s + \frac{L}{2\pi}\xi_c\right) - y_0 n_{z0}\right]\cos\gamma_m.$$

2.5. Mathematical model for generated spiral bevel and hypoid gear surfaces

Note that the roll ratio, η_a, between the cradle and workpiece is a function of the cradle roll angle, ξ_c, as shown in equation (1). Substituting equation (22) into equation (23), one obtains the locus of the imaginary generating gear represented in the workpiece coordinate system. The tooth surfaces of the generated spiral bevel and hypoid gears are determined by considering equations (23) and (27) simultaneously.

3. EXAMPLE

In this section, a spiral bevel gear set generated using a Gleason no. 463 hypoid grinder is used as an example to demonstrate application of the proposed mathematical model and verify its accuracy. The gear blank dimensions and grinding wheel specifications are given in Table 1, and the machine settings are shown in Table 2. The gear was finished using the duplex grind (i.e. spread blade) process while the pinion was ground side-by-side using different machine settings (i.e. fixed settings).

The theoretical tooth surfaces calculated by the proposed mathematical model can be regarded as the tooth geometry standard for inspecting finished spiral bevel and hypoid gears. With the aid of the proposed mathematical model, the continuous bevel gear tooth surface is discretized into $m \times n$ sampling points, using a mapping method as shown in Fig. 6. The values of m and n depend on the tooth surface geometry, sampling accuracy, machine precision as well as product requirements. The sampling surface points are numbered in ascending order from toe to heel, and root to face. The coordinates of the theoretical sampling points are down-loaded to the CNC coordinate measuring machine. Using the down-loaded data, the CNC coordinate measuring machine measures the relative points on the real cut tooth surface. The measured data are then compared with the theoretical data and any deviations are calculated.

Comparisons of the tooth topographies, obtained from the mathematical model and measured data from real cut gears, are shown in Figs 7–9. Since the convex and concave pinion sides were ground side-by-side with different machine settings, Figs 7 and 8 show the surface deviation comparisons between the theoretical pinion surfaces and the convex and concave side surfaces of the real cut pinion, respectively. The maximum surface deviations are 0.013 mm on the convex side and 0.023 mm on the concave side, respectively. A comparison of surface deviations between the theoretical spiral bevel gear surface and the real cut gear surface finished by duplex grinding is shown in Fig. 9. The tooth thickness deviation at reference point E3 is 0.023 mm and the maximum surface deviation is about 0.005 mm. Therefore, the tooth surfaces generated by the proposed mathematical model are quite consistent with those of real cut gears. This indicates that the modified roll motion during grinding was successfully simulated by the proposed mathematical model.

Tooth contact patterns and kinematic errors in the sprial bevel and hypoid gears were simulated using the proposed mathematical model and tooth contact analysis (TCA) program; the results are shown in Fig. 10. The quadrangles formed by the solid lines indicate, respectively, the spiral bevel gear and pinion teeth boundaries. The thick solid line traces the contact point path. The solid-line ellipses show the single-tooth-pair instantaneous contact mesh zones, and the dotted-line ellipses show the multiple-tooth-pair mesh zones. The dotted lines drawn within the quadrangles indicate

Table 1. Gear blank and grinding wheel used in the example

Items	Pinion	Gear
Blank data		
Number of teeth	27	28
Face width	25.000 mm	25.000 mm
Pitch angle	22° 4′	22° 56′
Outside diameter	128.725 mm	132.911 mm
Pitch apex to crown	148.381 mm	147.452 mm
Grinding wheel specifications		
Mean dia. of grinding wheel	—	250.000 mm
Point dia. of grinding wheel (I.B.)	250.952 mm	—
Point dia. of grinding wheel (O.B.)	251.460 mm	—
Inside blade angle	21° 0′	21° 0′
Outside blade angle	19° 0′	19° 0′
Point width	—	2.413 mm
Tip fillet	1.088 mm	0.048 mm

Table 2. Machine settings used in the example

Machine settings	Pinion I.B.	Pinion O.B.	Gear
Machine root angle	20° 26′	20° 26′	21° 15′
Machine center to back	−9.013 mm	−8.463 mm	−2.402 mm
Sliding base	3.146 mm	2.964 mm	0.870 mm
Blank offset	−11.642 mm	−11.275 mm	2.957 mm
Cam setting	101.600 mm	101.600 mm	76.200 mm
Eccentric angle	32° 49′	32° 38′	35° 44′
Cradle angle	67° 3′	71° 45′	324° 59′
Cam guide angle	5° 10′	0° 0′	−0° 40′
Feed cam setting	6° 0′	0° 0′	0° 0′
Generating cam no.	#23	#23	#29
Index interval	10	10	9
Index gears	48/80 × 50/81	48/80 × 50/81	42/70 × 45/84

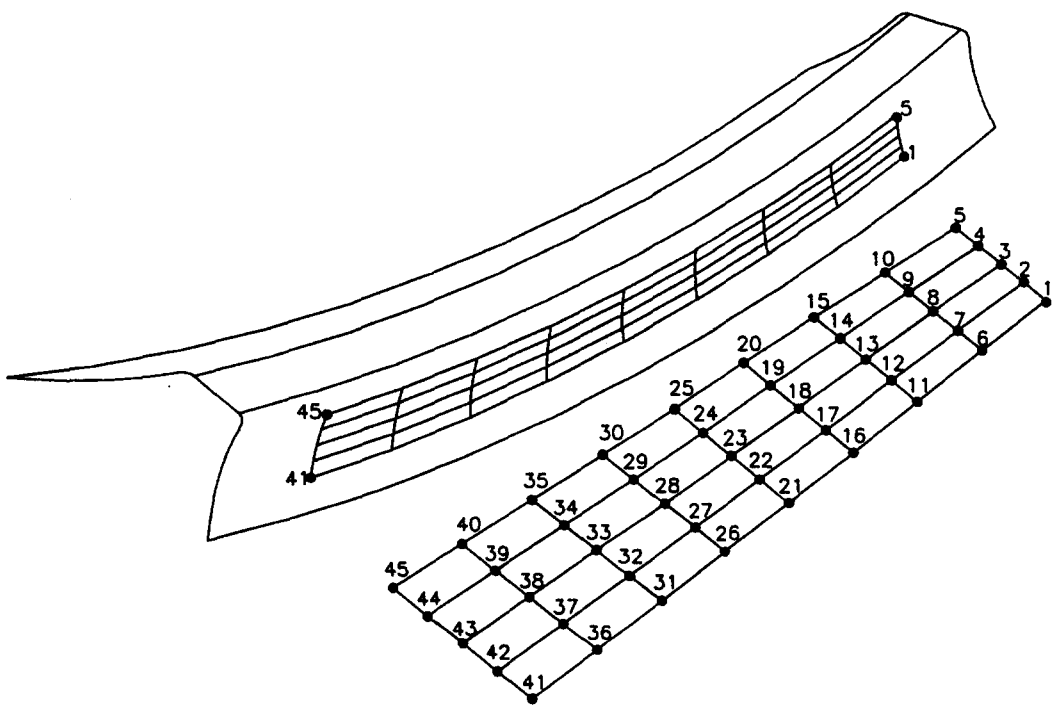

Fig. 6. Sampling surface points on the spiral bevel gear convex side.

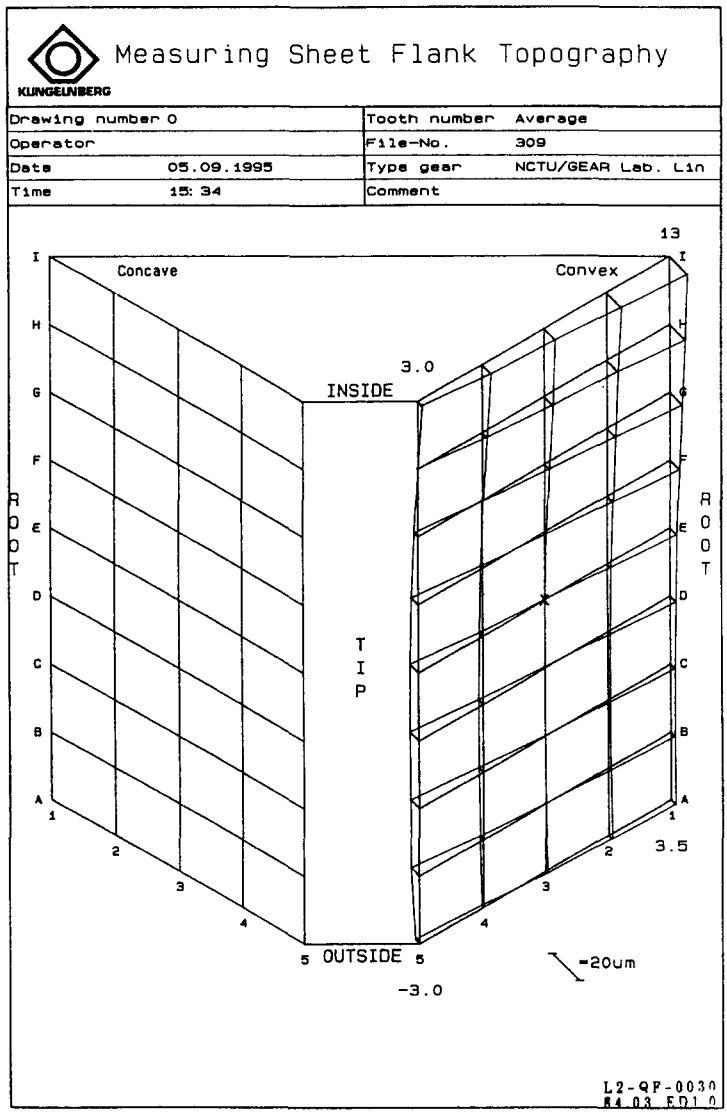

Fig. 7. Comparison of theoretical data with measured data for pinion convex side.

the tooth work-surface boundaries generated by the grinding wheel's straight-line generatrix. In this example, the bearing contacts are located in the center region of the tooth face with a slight "bias in" contact pattern. The kinematic errors are 9.49 arc-seconds on the pinion convex side and 9.91 arc-seconds on the pinion concave side.

4. CONCLUSION

The proposed mathematical model was divided into four main kinematic modules: grinding wheel surface geometry, modified roll generating train, spatial relationship between grinding wheel and workpiece and equation of meshing that simulates the generation process. Tooth surfaces obtained by the proposed mathematical model can be considered the tooth geometry standard for inspecting spiral bevel and hypoid gears manufactured using the modified roll method. Variation in roll ratio between the imaginary generating gear and generated gear during the generation process has also been taken into consideration. Since the proposed mathematical model was developed in terms of actual manufacturing machine-tool settings and machine constants, it is therefore very easy to implement it and to establish a closed loop manufacturing system for spiral bevel and hypoid gears. Computer programs such as the TCA program, computer-aided CNC inspection program, and corrective machine-tool settings calculation program have been developed

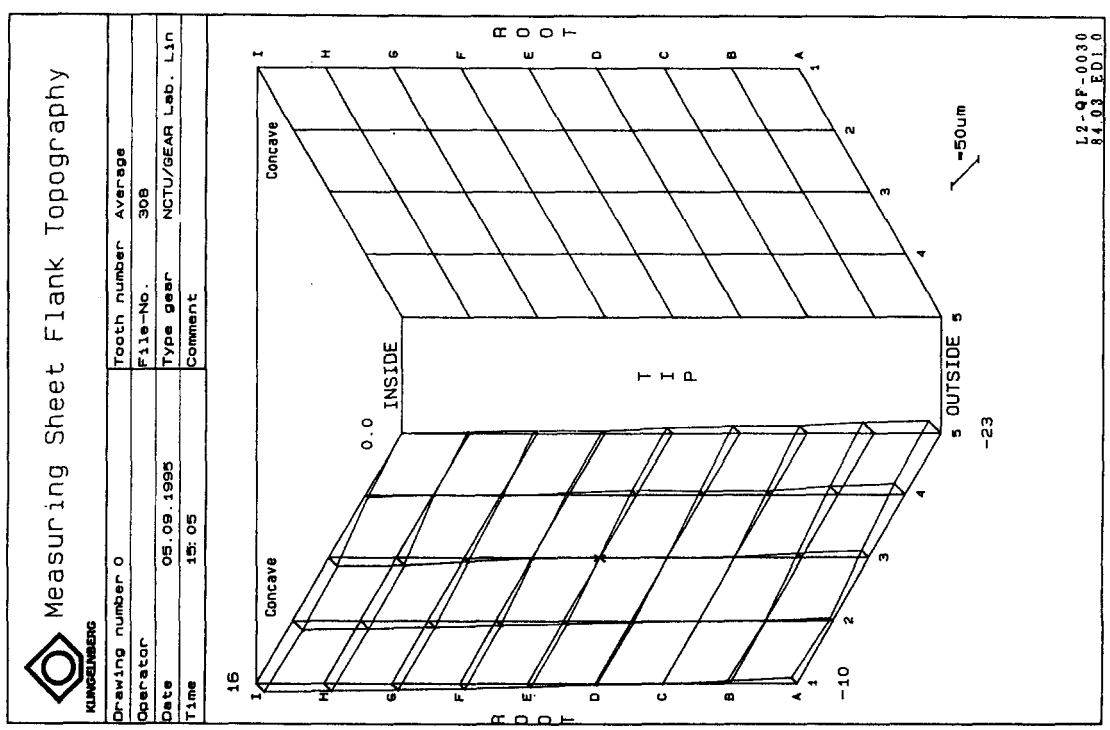

Fig. 8. Comparison of theoretical data with measured data for pinion concave side.

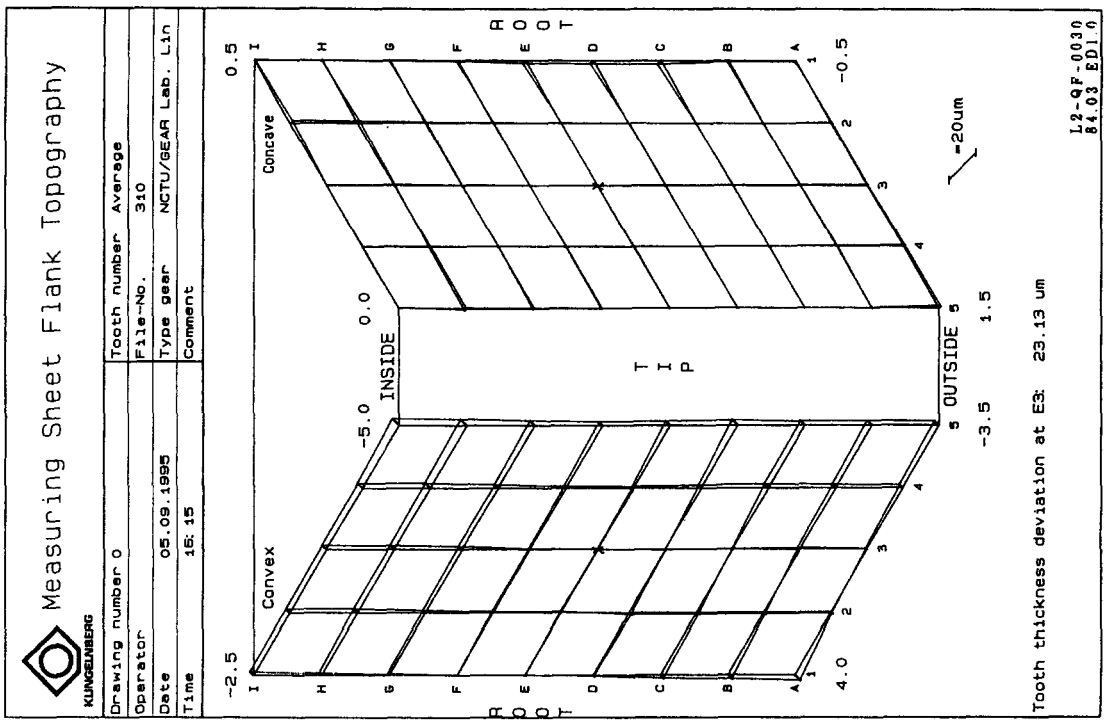

Fig. 9. Comparison of theoretical data with measured data for spiral bevel gear.

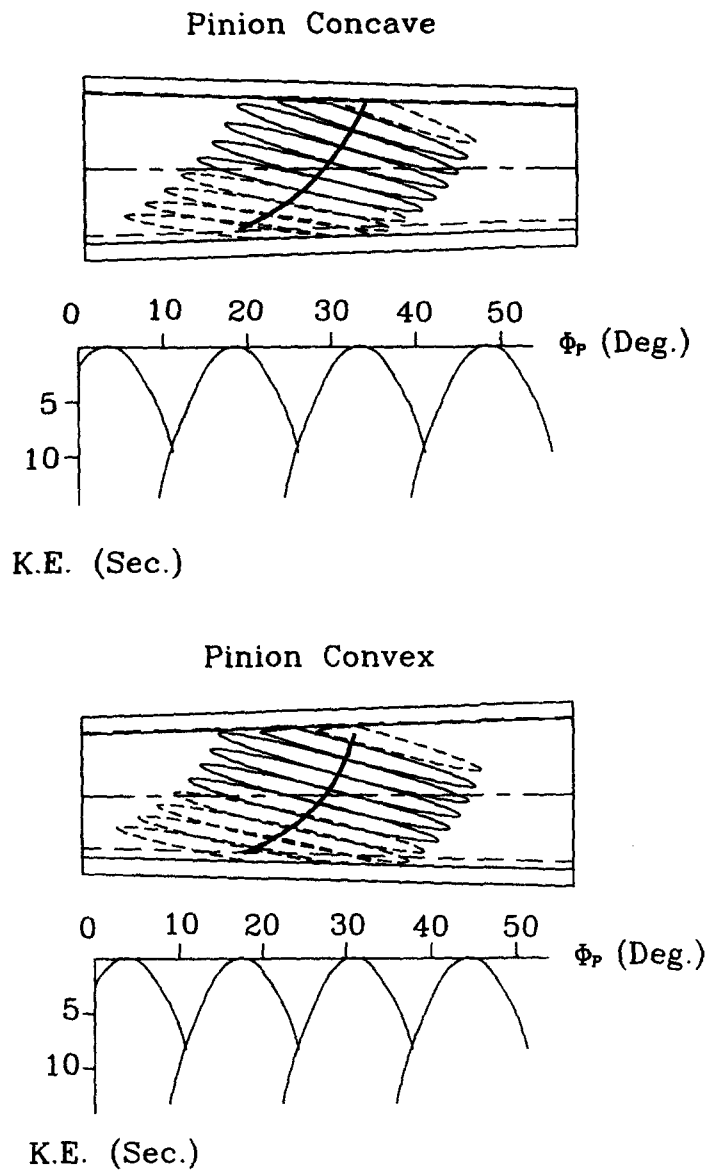

Fig. 10. Bearing contacts and kinematic errors of the sprial bevel gear set.

and used successfully to form such closed loop manufacturing system. The results of this paper can be applied to improve the quality and quantity controls for the manufacture of sprial bevel and hypoid gears.

Acknowledgement—The authors are grateful to the National Science Council of the R.O.C. for their grant. Part of this work was performed under contract no. NSC-84-2212-E-009-018.

REFERENCES

1. Gleason Works, *Theory and Tooth Contact of Helixform Analysis*. New York, 1965.
2. Baxter, M. L., *AGMA paper*, 1966, 139.
3. Litvin, F. L. and Gutman, Y., *ASME Journal of Mechanical Design*, 1981, **103**, 83.
4. Huston, R. L. and Coy, J. J., *ASME Journal of Mechanical Design*, 1981, **103**, 127.
5. Huston, R. L., Lin, Y. and Coy, J. J., *ASME Journal of Mechanical Design*, 1983, **105**, 132.
6. Tsai, Y. C. and Chin, P. C., *ASME Journal of Mechanism and Transmissions Automation Design*, 1987, **111**, 443.
7. Litvin, F. L., Zhang, Y., *et al.*, *ASME Journal of Mechanism Transmissions Automation Design*, 1988, **110**, 495.
8. Fong, Z. H. and Tsay, C. B., *ASME Journal of Mechanical Design*, 1991, **113**, 174.
9. Fong, Z. H. and Tsay, C. B., *ASME Journal of Mechanical Design*, 1991, **113**, 346.

10. Fong, Z. H. and Tsay, C. B., *ASME Journal of Mechanical Design*, 1992, **114,** 498.
11. Fong, Z. H. and Tsay, C. B., *ASME Journal of Mechanical Design*, 1992, **114,** 317.
12. Gleason Works, *Phoenix Closed Loop System*. New York, 1991.
13. M&M Precision System, *The CNC Gear Inspection System for the Spiral Bevel Gears-QC 3000 Manual*, Ohio, 1990.
14. Klingelnberg Soehne, *The CNC Inspection System for the Spiral Bevel Gears–HP-KEG Software Manual*, Remscheid, Hueckeswagen Factory, Germany, 1990.
15. Lemanski, A. J., AGMA paper 85FTM10, 1995.
16. Krenzer, T. J., AGMA paper 84FTM4, 1994.
17. Litvin, F. L., Zhang, Y., *et al.*, *ASME Journal of Mechanical Design*, 1991, **113,** 55.
18. Litvin, F. L., Kuan, C., *et al.*, *ASME Journal of Mechanical Design*, 1993, **115,** 995.
19. Zhang, Y. and Litvin, F. L., *ASME Journal of Mechanical Design*, 1994, **116,** 677.
20. Gleason Works, *Gear Process Theory*, New York, 1971.
21. Gleason Works, *Calculation Instructions–Generated Spiral Bevel Gears, Fixed Setting Method for Finishing Pinions for Machines with Modified Roll–SGM*. New York, 1971.
22. Litvin, F. L., *Theory of Gearing*, NASA, Washington, DC, 1989, p. 358.
23. Shtipelman, B. A., *Design and Manufacture of Hypoid Gears*. Wiley, New York, 1978, p. 125.